Levitation, Lift, and Bidirectional Motion of Colloidal Particles in an Electrically Driven Nematic Liquid Crystal

O. P. Pishnyak, S. Tang, J. R. Kelly, S. V. Shiyanovskii, and O. D. Lavrentovich

Liquid Crystal Institute and Chemical Physics Interdisciplinary Program, Kent State University, Kent, Ohio 44242, USA
(Received 30 April 2007; published 21 September 2007)

We study electric-field-induced dynamics of colloids in a nematic cell, experimentally and by computer simulations. Solid particles in the nematic bulk create director distortions of dipolar type. Elastic repulsion from the walls keeps the particles in the middle of cell. The ac electric field reorients the dipoles and lifts them to top or bottom, depending on dipole orientation. Once near the walls, the colloids are carried along two antiparallel horizontal directions by nematic backflow. Computer simulations of the backflow agree with the experiment.

Colloidal dispersions with a liquid crystal (LC) component are a fascinating class of soft matter, in which the equilibrium is often achieved by introducing topological defects in the director field $\hat{\mathbf{n}}(\mathbf{r})$, stabilized by surface anchoring at interfaces [1,2]. Recently, a number of interesting dynamic effects have been reported for these materials [3–13]. The topic is complex, as the hydrodynamics of LCs themselves is non-Newtonian and anisotropic; adding colloids brings an even higher level of complexity. For example, gradients of the director field [12] or the scalar order parameter [13] create forces driving the particles, while the viscous flow can modify $\hat{\mathbf{n}}(\mathbf{r})$ around an inclusion [5,10].

The central question, the role of $\hat{\mathbf{n}}(\mathbf{r})$ in the dynamics of colloidal particles in a LC, is poorly understood and was not addressed in the previous experimental studies (except for the case of smectic LC [8]). In this Letter, we use fluorescence confocal polarizing microscopy (FCPM) [14] to track both the 3D $\hat{\mathbf{n}}(\mathbf{r})$ around the particles and their motion caused by the ac electric field in a flat nematic cell. We discover a surprising bidirectional motion: half of the particles move to the top plate and then migrate along one horizontal direction, while the other half move to the bottom and migrate in the opposite direction. The polarity of director distortions determines the direction of lift force. The particle horizontal velocity agrees well with the simulated velocity profile of backflow. As an auxiliary result, we quantify the elastic interactions of a particle with the bounding walls, causing levitation of the particle.

We used a nematic LC E7 (EM Industries, Inc.) doped with 0.01 wt% of fluorescent dye *N, N'*-Bis(2,5-di-tert-butylphenyl)-3,4,9,10-perylenedicarboximide (BTBP, Sigma-Aldrich). In FCPM, the 3D director $\hat{\mathbf{n}}(\mathbf{r})$ is visualized by measuring the intensity of fluorescence of BTBP molecules; it is maximum when the polarization of probing light is parallel to the local $\hat{\mathbf{n}}$ [14]. Spherical silica particles of diameter $2R \approx 4.1 \pm 0.4$ μm (Bangs Laboratories, Inc., Catalog No. SS05N, Lot No. 6725) were added to E7 at concentration ~ 0.5 wt%. The cells were formed by glass plates covered with transparent indium tin oxide

electrodes and rubbed polyimide PI2555 (Microsystems) alignment layers that produce a uniaxial alignment of $\hat{\mathbf{n}}$ with a small pretilt angle $\theta \approx 2°$, i.e., $\hat{\mathbf{n}} \approx (1, 0, 0)$ in the Cartesian coordinates with the axis x at the bottom plate and the axis z perpendicular to it, Fig. 1.

All the experiments were performed at 21 °C. At the particle surface, $\hat{\mathbf{n}}$ is anchored normally [15]. To match the surrounding uniform director, each particle is accompanied by a hyperbolic point defect hedgehog, so that the overall $\hat{\mathbf{n}}(\mathbf{r})$ is of dipolar symmetry [1], Fig. 1(a) and 1(b). The dipole **p** is directed from the hedgehog towards the sphere. The particles "levitate", Fig. 1(a)–1(e), as gravity is balanced by wall-dipole elastic repulsion. The repulsion potential for two side-by-side parallel dipoles separated by r is $E = 4\pi K p^2/r^3$, $p = AR^2$ [1], so the balance of forces acting on the particle writes

$$F = F_0 - F_h - F_g$$
$$= \frac{3}{2}\pi K A^2 \left(\frac{2R}{h - 2\delta}\right)^4 - \frac{3}{2}\pi K A^2 \left(\frac{2R}{h + 2\delta}\right)^4$$
$$- \frac{4}{3}\pi R^3 (\rho_p - \rho)g$$
$$= 0. \tag{1}$$

Here F_0 is the repulsion force between the dipole and its mirror image with respect to the bottom plate $z = 0$; F_h is a similar force for the top plate $z = h$; h is the cell thickness; δ is the downward shift of the particle from $z = h/2$; $\rho_p - \rho \sim 0.98 \times 10^3$ kg/m^3 is the difference in the densities of silica and E7; $K \approx 15$ pN is the average of splay $K_1 = 11.7$ pN and bend $K_3 = 19.5$ pN constants of E7 [16]; $A = 2.04$ is the numerical factor [17]; $g = 9.8$ m/s^2 is the standard gravity. Theoretical prediction (1) for $\delta(h)$ agrees well with the experiment, Fig. 1(c). In the rest of the work, we used cells with $h = 19$–21 μm, in which $\delta \leq 1$ μm.

Application of an ac electric voltage U reorients $\hat{\mathbf{n}}$ along the z axis and lifts the particles towards one of the plates, Fig. 1(f) and 1(g). Because of the pretilt, $\hat{\mathbf{n}}$ reorients counterclockwise. Particles with $p_x < 0$ lift to the top, while $p_x > 0$ move to the bottom; the hedgehogs are closer
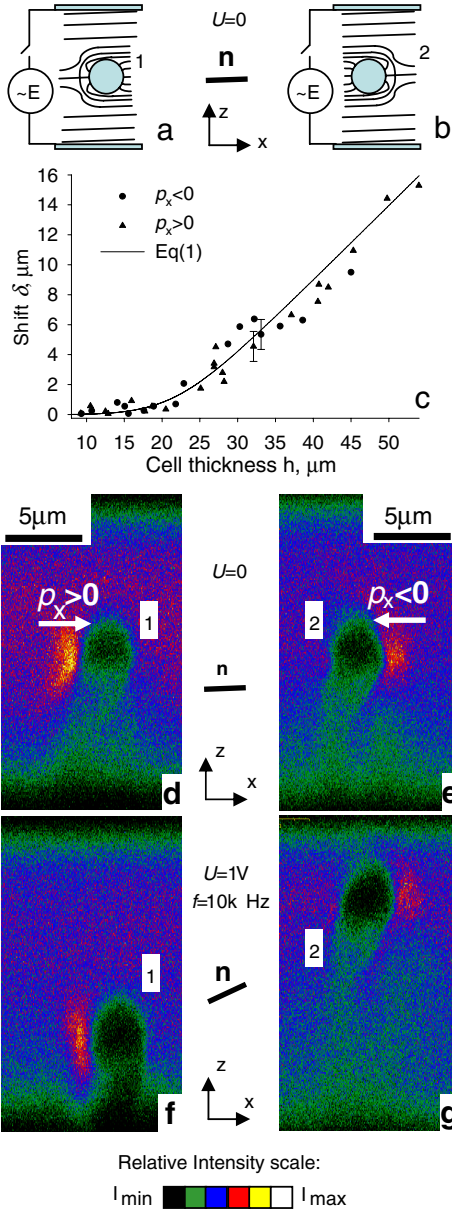
FIG. 1 (color online).   Elastic dipoles formed by colloids 1 (a) and 2 (b) in the cell with $h = 19\ \mu m$, and their FCPM textures (d), (e). Part (c) shows the experimental and theoretical (solid line) shift δ of the particles from $z = h/2$ as a function of h. The ac field reorients $\hat{\mathbf{n}}$ and pushes particle 1 to the bottom (f) and particle 2 to the top (g). In FCPM textures (d)–(g), light polarization is normal to the plane of figures.

to the wall and the spheres are farther away. The rate of the voltage envelope increase was set low, 0.1 V/s (in order to minimize the transient backflow), but the carrier frequency was high, $f = 10$ kHz (to avoid electrohydrodynamics caused by ions). With the typical ionic mobility $\mu \sim 10^{-10}$ m^2 s^{-1} V^{-1} [18], the maximum shift of ions during one quarter of the ac field period is small, $\delta_i \sim \sqrt{\mu U / 4f} \sim 0.1\ \mu m$ for $U = 4$ V. The observed particles shift is thus associated mostly with elastic interaction between **p** and polar splay-bend caused by the electric

field near the walls and also possibly with the flexoelectric polarization [2] and its coupling to ions in the cell.

The voltage-induced distortions of $\hat{\mathbf{n}}$ concentrate near the walls, over the length $\xi = \frac{h}{U}\sqrt{\frac{K}{\varepsilon_0(\varepsilon_{||}-\varepsilon_\perp)}}$, and can additionally trap the particles. Here, $\varepsilon_0 = 8.9$ pN/V^2 and $\varepsilon_{||} - \varepsilon_\perp \approx 14.5$ is the dielectric anisotropy of E7 [16]; $\xi \approx 2\ \mu m$ for $U = 3$ V. By moving the particle from the uniform central part to the wall, one reduces the elastic energy by $\sim KR^3/\xi^2$ [12]. The corresponding trap force $F_{trap} \sim KR^3/\xi^3 \sim K \sim 10$ pN is significant, as compared to $F_h \approx 0.3$ pN, $F_0 \approx 0.6$ pN, calculated from Eq. (1) for $h = 21\ \mu m$. Experimentally, the distance between the particle surface and the wall is $\sim 2\ \mu m$ for $U = 3$ V. The lift and trap forces that keep the particles near the walls allow one to use the LC backflow effects, i.e., material flow caused by director reorientation, for a well controlled microfluidic manipulation, Fig. 2. The transport of particles is possible only if the net flow is nonzero, which indeed happens near the walls, as shown in the experiment and simulations below. Furthermore, one can expect that the horizontal shift of particles would depend on the duration of the voltage on and off states [6].

We created the backflow by applying a voltage $U = 10$ V, $f = 10$ kHz, modulated with a frequency $f_m = 0.5$–100 Hz (following the lift-creating pulse described above). The duty ratio defined as the duration of the field on to the total duration of the field cycle was 50%. We used the generator DS345 (Stanford Research Systems, Inc.). The particles are carried bidirectionally: those near the top
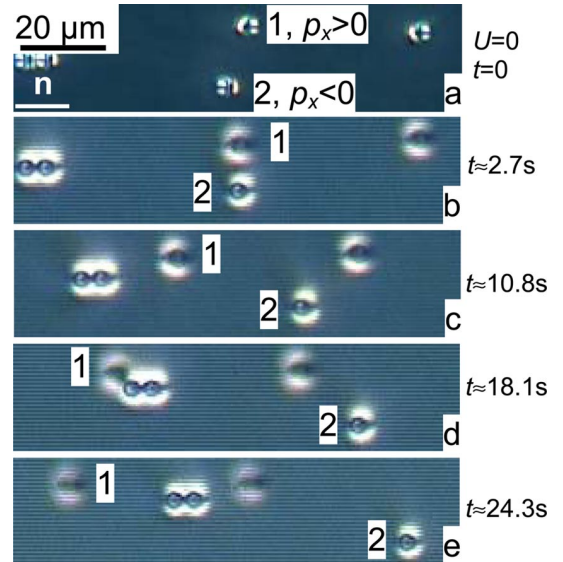

FIG. 2 (color online).   Electric-field-induced bidirectional motion of particles 1 and 2: (a) initial state, $U = 0$, particles at $z = h/2$; (b)–(e) bidirectional motion driven by $U = 10$ V, $f = 10$ kHz, $f_m = 10$ Hz. Particle 1, near the bottom wall, migrates to the left $(-x)$, while particle 2, near the top, moves to the right $(+x)$. The particles of type 1 and 2 are well separated along the z axis and do not trap each other; t is the time since voltage application.

move towards $+x$ and those near the bottom move towards $-x$; in both cases, the hedgehog leads the way. The motion is similar to the one observed by Ref. [9], with that difference that in our case it is bidirectional rather than a unidirectional. The average velocity of particles $\langle v_p \rangle$ depends on f_m nonmonotonously, with a maximum at $f_m \approx 5$ Hz, Fig. 3(a). The particles may stick together and form chains 2–3 spheres long; the speed of these chains does not differ much from the speed $\langle v_p \rangle$ of single colloids, compare the two-particle cluster and particle 2 in Fig. 2(b)–2(e). This feature suggests that the particles are driven predominantly by the backflow effect. A video of bidirectional dynamics is available; see supplementary material [19].

We performed numerical simulations of the electrically driven flow using the Ericksen-Leslie model [2], for $U = 10$ V, $h = 21$ μm, pretilt $2°$, and viscosity coefficients of E7 [16] $\alpha_1 = -21$, $\alpha_2 = -282$, $\alpha_3 = -1$, $\alpha_4 = 225$, $\alpha_5 = 92$, $\alpha_6 = -191$ (all in mPa s units). We assume that $\hat{\mathbf{n}} = (\cos\theta(z, t), 0, \sin\theta(z, t))$ is in the xz plane, and that the hydrodynamic flow has only an x component, $\mathbf{v} = \{v(z, t), 0, 0\}$. We neglect the flow inertia term, because the flow relaxation time $\tau_v \approx \rho h^2/\pi^2 \alpha_4 \sim 1$ μs is much shorter than the director relaxation times $\tau_{\text{on}} \approx (\alpha_3 - \alpha_2)h^2/\varepsilon_0(\varepsilon_\parallel - \varepsilon_\perp)U^2 \sim 10$ ms and $\tau_{\text{off}} \approx (\alpha_3 - \alpha_2)h^2/\pi^2 K_1 \sim 1$ s, and we write the Ericksen-Leslie equations as

$$(\alpha_3 - \alpha_2)\dot{\theta} = -G_\theta - (\alpha_3\cos^2\theta - \alpha_1\sin^2\theta)v', \quad (2)$$

$$(\alpha_3\cos^2\theta - \alpha_2\sin^2\theta)\dot{\theta} + \tilde{\alpha}(\theta)v' = \sigma_{zx}(t), \quad (3)$$

where the dot and prime denote the time and z derivatives, respectively; $\tilde{\alpha}(\theta) = \frac{1}{2}[\frac{1}{2}\alpha_1\sin^2 2\theta + (\alpha_5 - \alpha_2)\sin^2\theta + \alpha_4 + (\alpha_3 + \alpha_6)\cos^2\theta]$; G_θ is the variational derivative of Frank-Oseen energy,

$$G_\theta = -(K_3\sin^2\theta + K_1\cos^2\theta)\theta'' - \frac{1}{2}(K_3 - K_1)\sin 2\theta\,\theta'^2$$
$$- \frac{1}{2}\varepsilon_0(\varepsilon_\parallel - \varepsilon_\perp)U^2 \sin 2\theta[I_1\tilde{\varepsilon}(\theta)]^{-2}, \quad (4)$$

with $I_1 = \int_0^d dz/\tilde{\varepsilon}(\theta)$, $\tilde{\varepsilon}(\theta) = \varepsilon_\parallel\sin^2\theta + \varepsilon_\perp\cos^2\theta$; $\sigma_{zx}(t)$ is the zx component of the nematic strain tensor that does not depend on z and is determined from the boundary condition $v(z = 0) = v(z = h) = 0$. We solve Eqs. (2) and (3) using an implicit Crank-Nicolson scheme for time derivatives [20].

The flow behavior is different for $f_m \ll \tau^{-1} = (\tau_{\text{on}} + \tau_{\text{off}})^{-1} \approx \tau_{\text{off}}^{-1} \approx 1$ Hz, when $\hat{\mathbf{n}}$ has time to equilibrate, and for $f_m \gtrsim \tau^{-1}$, when $\hat{\mathbf{n}}$ does not equilibrate. The regime $f_m \ll \tau^{-1}$ is well studied [18]. When the field is switched on, a counterclockwise rotation of $\hat{\mathbf{n}}$ causes a flow with $v_{\text{on}}(h/2 < z < h) < 0$ and $v_{\text{on}}(0 < z < h/2) > 0$. With time, this flow gradually vanishes. The symmetry $\theta(z) = \theta(h - z)$ and $v(z) = -v(h - z)$ allows us to discuss the bottom half only. The flow-produced displacement $s_{\text{on}}(0 < z < h/2) > 0$ of fluid is maximum, $s_{\text{on}} \approx 1.2$ μm, at $z \approx 2$ μm. When the field is switched off, the fluid displacement is larger and of opposite sign, $s_{\text{off}} \approx -3.7$ μm for

$z \approx 2$ μm. The total displacement per one cycle is negative, $s_{\text{total}} = s_{\text{on}} + s_{\text{off}} \approx -2.5$ μm. The particles near the bottom are thus pushed towards $(-x)$, and those near the top move towards $+x$. For a low f_m, the average velocity of the fluid $\langle v \rangle = s_{\text{total}}f_m$ increases linearly with f_m, in agreement with the data on $\langle v_p \rangle \approx \langle v \rangle$, Fig. 3(a).

When $f_m \gtrsim \tau^{-1}$, equilibration after each on and off switch is not complete and the picture is very different, Fig. 4. Both s_{on} and s_{off} initially become shorter and then switch signs, but their sum $s_{\text{total}} = s_{\text{on}} + s_{\text{off}}$ remains negative, Fig. 3(b). In the limit $f_m \to \infty$, small back and forth reorientations cancel each other so that $\langle v \rangle \to 0$. The dependence $\langle v \rangle(f_m)$ is nonmonotonous, with $\langle v \rangle \to 0$ for low and high f_m's and a maximum for an intermediate f_m. This is exactly what we observe in the experiment for $\langle v_p \rangle(f_m)$, Fig. 3(a). Good agreement suggests that the prime mechanism of the particle migration in our experiments is the backflow effect.

Our system is flexible in terms of controlling the particle behavior. For the same direction of the elastic dipoles, the lifting force and direction of migration can be reversed by
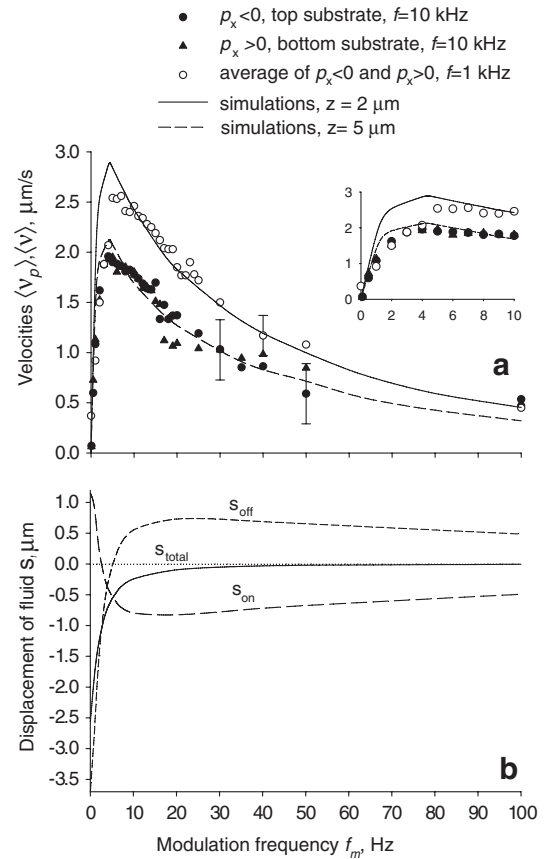

- $p_x < 0$, top substrate, $f = 10$ kHz
- $p_x > 0$, bottom substrate, $f = 10$ kHz
- average of $p_x < 0$ and $p_x > 0$, $f = 1$ kHz
— simulations, $z = 2$ μm
--- simulations, $z = 5$ μm

FIG. 3.   (a) Average particle velocity $\langle v_p \rangle$ vs f_m for $f = 10$ kHz (filled symbols) and $f = 1$ kHz (open symbols). The lines show the simulated average backflow velocity $\langle v \rangle(f_m)$, at $z = 2$ μm and 5 μm. The inset shows the enlarged plot for $0 < f_m \leq 10$ Hz; (b) simulated displacement following the switch on (s_{on}), switch off (s_{off}), and during an entire cycle, on + off (s_{total}), for $z = 2$ μm.
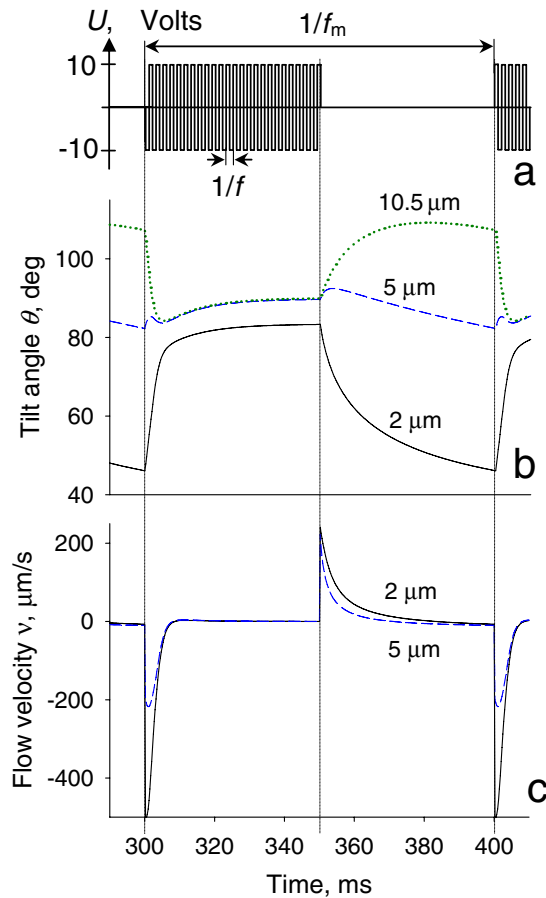
FIG. 4 (color online). Computer-simulated dynamics of the director tilt (b) and instantaneous velocity v (c) of backflow caused by a voltage $U = 10$ V, $f = 10$ kHz, $f_m = 10$ Hz (a).

altering the voltage increase rate and frequency. Such a reversal is observed when one applies 10 V with a high rate of 3.5×10^3 V/s at $f = 1$ kHz; the velocities $\langle v_p \rangle$ remain close to the ones in previous case, Fig. 3(a) (open symbols).

To conclude, the colloidal dynamics in the nematic LC is controlled by director distortions. We demonstrated lift forces that move the particles vertically and backflow that moves them horizontally. The lift forces in a LC are not limited by elasticity and can also be caused by hydrodynamic effects known for isotropic fluids, namely, the Saffman lift [21], $F_S \approx 6.46 \, \bar{\alpha} R^2 v \sqrt{\dot{\gamma} \rho / \bar{\alpha}}$ ($\bar{\alpha}$ is a typical viscosity, $\dot{\gamma}$ is the shear rate), arising from the flow inertia and by the combined effect of the wall presence and particle nonsphericity or deformability [22], $F_{ns} \sim \bar{\alpha} \, \dot{\gamma} R^2 \varphi(R/z)$, where φ is a dimensionless function of the particle shape, size, and the distance z to the wall. For $\bar{\alpha} \sim 0.2$ Pa s, $\dot{\gamma} \sim 50$ s^{-1}, and $\varphi \sim 1$ [in LC, nonsphericity should be related to $\hat{\mathbf{n}}(\mathbf{r})$ rather than to the particle shape itself], these forces can be significant, $F_S \sim 1$ pN, $F_{ns} \sim 40$ pN. Note also that high backflow velocity, $v \gtrsim 50 \, \mu$m/s, can make the Ericksen number (the ratio of elastic and viscous torques), $\text{Er} = \frac{\bar{\alpha} |v| R}{K}$, larger than 1 and

thus modify $\hat{\mathbf{n}}(\mathbf{r})$ [5,10]. Therefore, the subject of colloidal dynamics in LCs holds a major promise in terms of diversity of physical phenomena, most of which are not clear at the moment. What is clear, however, is that the described unique bidirectional motion of particles offers an opportunity for experimental studies of systems far from equilibrium, such as driven diffusion systems, see, e.g., [23]. These studies are in progress.

[1] P. Poulin *et al.*, Science **275**, 1770 (1997).
[2] M. Kleman and O. D. Lavrentovich, *Soft Matter Physics: An Introduction* (Springer-Verlag, New York, 2003).
[3] R. W. Ruhwandl and E. M. Terentjev, Phys. Rev. E **54**, 5204 (1996).
[4] H. Stark, D. Ventzki, and M. Reichert, J. Phys. Condens. Matter **15**, S191 (2003).
[5] J.-I. Fukuda *et al.*, J. Phys. Condens. Matter **16**, S1957 (2004).
[6] Y. Mieda and K. Furutani, Appl. Phys. Lett. **86**, 101901 (2005).
[7] Y. Mieda and K. Furutani, Phys. Rev. Lett. **95**, 177801 (2005).
[8] G. Liao *et al.*, Phys. Rev. E **72**, 031704 (2005).
[9] I. Dierking, G. Biddulph, and K. Matthews, Phys. Rev. E **73**, 011702 (2006).
[10] T. Araki and H. Tanaka, J. Phys. Condens. Matter **18**, L193 (2006).
[11] A. Fernandez-Nieves *et al.*, Phys. Rev. Lett. **98**, 087801 (2007).
[12] D. Voloschenko *et al.*, Phys. Rev. E **65**, 060701(R) (2002).
[13] J. West *et al.*, Eur. Phys. J. E **20**, 237 (2006).
[14] I. I. Smalyukh, S. V. Shiyanovskii, and O. D. Lavrentovich, Chem. Phys. Lett. **336**, 88 (2001).
[15] In some samples with recently purchased E7 (Jan 2007) the anchoring was tangential. In this work, we used only samples with strong normal anchoring evidenced by the presence of hyperbolic hedgehog near the sphere.
[16] H. Wang *et al.*, Liq. Cryst. **33**, 91 (2006).
[17] T. C. Lubensky *et al.*, Phys. Rev. E **57**, 610 (1998).
[18] L. M. Blinov and V. G. Chigrinov, *Electro-Optic Effects in Liquid Crystal Materials* (Springer-Verlag, New York, 1994).
[19] See EPAPS Document No. E-PRLTAO-99-059736 for video of bidirectional dynamics of colloidal particles. For more information on EPAPS, see http://www.aip.org/pubservs/epaps.html.
[20] J. Crank and P. Nicolson, Proc. Cambridge Philos. Soc. **43**, 50 (1947).
[21] H. Stone, J. Fluid Mech. **409**, 165 (2000).
[22] M. Abkarian, C. Lartigue, and A. Viallat, Phys. Rev. Lett. **88**, 068103 (2002).
[23] I. T. Georgiev, B. Schmittmann, and R. K. P. Zia, Phys. Rev. Lett. **94**, 115701 (2005).